This is a pre print version of the following article:

Perfect chiral quantum routing / Cavazzoni, Simone; Ragazzi, Giovanni; Bordone, Paolo; Paris, Matteo G. A.. - In: PHYSICAL REVIEW A. - ISSN 2469-9926. - 111:(2025), pp. 032439-1-032439-7. [10.1103/PhysRevA.111.032439]

Terms of use:

The terms and conditions for the reuse of this version of the manuscript are specified in the publishing policy. For all terms of use and more information see the publisher's website.

03/05/2026 09:17

(Article begins on next page)

arXiv:2406.11834v1 [quant-ph] 17 Jun 2024

Perfect Chiral Quantum Routing

Simone Cavazzoni,[1,*] Giovanni Ragazzi,[1,†] Paolo Bordone,[1,2,‡] and Matteo G. A. Paris[3,4,§]

[1] *Dipartimento di Scienze Fisiche, Informatiche e Matematiche, Università di Modena e Reggio Emilia, I-41125 Modena, Italy*
[2] *Centro S3, CNR-Istituto di Nanoscienze, I-41125 Modena, Italy*
[3] *Quantum Technology Lab, Dipartimento di Fisica* Aldo Pontremoli, *Università degli Studi di Milano, I-20133 Milano, Italy*
[4] *INFN, Sezione di Milano, I-20133 Milano, Italy*

(Dated: June 18, 2024)

Routing classical and quantum information is a fundamental task for most quantum information technologies and processes. Here, we consider information encoded in the position of a quantum walker on a graph, and design an optimal structure to achieve perfect quantum routing exploiting chirality and weighting of the edges. The topology, termed the *Lily Graph*, enables perfect (i.e., with fidelity one) and robust routing of classical (localized) or quantum (superposition) states of the walker to n different, orthogonal, spatial regions of the graph, corresponding to the n possible outputs of the device. The routing time is independent of the input signal and the number of outputs, making our scheme a robust and scalable solution for quantum networks.

Introduction – Routing of information is a fundamental procedure, crucial for any classical or quantum information protocol [1–8]. Networks that exchange information across different devices have to be equipped with a mechanism for selecting paths through the network itself [9–13]. Since quantum mechanics relies on probability amplitudes and interference patterns, the main challenge of this approach is to create a universal scheme that takes an initial state $|\psi_0\rangle$ and evolves it in different possible orthogonal states $|\psi_f\rangle$, according to some tunable parameters of the system, with unit probability at a time t^*. The orthogonality condition guarantees the perfect discriminability of the different $|\psi_f\rangle$. This condition can be implemented associating to $|\psi_0\rangle$ different states $|\psi_f\rangle$ belonging to separated spatial regions. In the following, we will refer to $|\psi_0\rangle$ as the *input* state and to $|\psi_f\rangle$ as an *output* state.

In this work, we consider information encoded in the position of a quantum walker on a graph [14, 15]. Routing this information means to drive the walker from a given input state to n possible output states by tuning a system parameter. Classical information corresponds to preparing the walker in a localized state, while quantum information may be encoded using superpositions of at least two localized states. We look for an optimal graph topology that ensures the routing of both classical and quantum information with unit fidelity in the shortest possible time. Indeed, by exploiting edge weighting and chirality, we have designed an optimal structure ensuring perfect routing. More specifically, using chirality alone, we achieve nearly optimal routing, while the combined use of chirality and edge weighting enables us to create a perfect router. This router achieves perfect (fidelity one) and robust routing in a time independent of the input signal and the number of outputs.

Ideal Quantum Router – An *ideal quantum router* is a system in which the time evolution, setting $\hbar = 1$, is governed by

$$e^{-iH\,t^*}\,|\psi_0\rangle = |\psi_f\rangle\,, \tag{1}$$

i.e. the time evolution operator acts as a projector $|\psi_f\rangle\langle\psi_0| + |\psi_0\rangle\langle\psi_f|$. An ideal quantum router should be able to carry not only classical information (for $|\psi_0\rangle$ and $|\psi_f\rangle$ being localized states) but quantum information as well (requiring $|\psi_0\rangle$ and $|\psi_f\rangle$ to be superpositions of localized states). Assuming that the system consists of a quantum walker on a graph, the time evolution of the system takes place in a position Hilbert space $\mathscr{H} = \mathrm{span}\{|x\rangle\}$. The states $|x\rangle$ are the sites of a $\mathcal{N}$ dimensional discrete space (i.e. a graph $\mathcal{G}(\mathcal{V}, \mathcal{E})$ of vertices $\mathcal{V}$ and edges $\mathcal{E}$). The discrete topology itself defines the adjacency matrix of the graph A, whose element A_{jk} are defined by the edges as

$$A_{jk} = \begin{cases} -1 & \text{if } j \neq k \text{ and } (j,k) \in \mathcal{E}, \\ 0 & \text{otherwise.} \end{cases} \tag{2}$$

which is a valid generator for the dynamics of a CTQW. Nonetheless, the quantumness of the system allows us to consider also chiral adjacency matrices [16–18]

$$C_{jk} = \begin{cases} e^{-i\phi_{jk}} & \text{if } j \neq k \text{ and } (j,k) \in \mathcal{E}, \\ 0 & \text{otherwise,} \end{cases} \tag{3}$$

defining a set of Hamiltonians generators $H = C = C^\dagger$ for quantum dynamics. Weighting the edges of the topology is also possible and corresponds to tuning the moduli of the elements of the Hamiltonian, e.g. setting $|H_{jk}| = \beta \in \mathbb{R}_+$.

Dimensionality reduction – In a quantum router, the quantities of interest are the probability amplitudes at particular vertices of the graph. Exploiting symmetries of the discrete structure, a dimensionality reduction method provides a tool to define an effective topology for the

time evolution of the system [19]. Considering a Taylor expansion of the quantum time evolution operator [20], the probability amplitude at a vertex $|\zeta\rangle$ can be expressed as

$$\begin{aligned}\langle\zeta|\, e^{-iHt}\,|\psi_0\rangle &= \sum_{k=0}^{\infty}\frac{(-it)^k}{k!}\,\langle\zeta|\, H^k\,|\psi_0\rangle \\ &= \langle\zeta|\, e^{-i\widetilde{H}t}\left|\widetilde{\psi}_0\right\rangle,\end{aligned} \tag{4}$$

where $\mathcal{P}H\mathcal{P} = \widetilde{H}$ is a reduced Hamiltonian, $\left|\widetilde{\psi}_0\right\rangle = \mathcal{P}\,|\psi_0\rangle$ is a reduced state, and $\mathcal{P}$ is the projector onto the Krylov subspace, which itself is defined as

$$\mathcal{K}(H,|\zeta\rangle) = \mathrm{span}(\{H^k\,|\zeta\rangle \mid k\in\mathbb{N}_0\}), \tag{5}$$

ensuring that $\left|\widetilde{\zeta}\right\rangle = \mathcal{P}\,|\zeta\rangle = |\zeta\rangle$. Clearly, $\dim\mathcal{K}(H,|\zeta\rangle) \leq \dim\mathscr{H} = \mathcal{N}$, as $\mathcal{K}(H,|\zeta\rangle) \subseteq \mathscr{H}$. The orthonormal basis for the subspace $\mathcal{K}(H,|\zeta\rangle)$ (i.e. $\{|e_1\rangle,\ldots,|e_m\rangle\}$) is built iteratively according to a Gram-Schmidt like orthonormalization procedure.

$$|u_k\rangle = |w_k\rangle - \sum_{j=1}^{k-1}\langle e_j|w_k\rangle\,|e_j\rangle \;\rightarrow\; |e_k\rangle = \frac{|u_k\rangle}{\sqrt{|u_k|^2}}, \tag{6}$$

with $|e_1\rangle = |\zeta\rangle$ and $H\,|e_{k-1}\rangle = |w_k\rangle$. The original problem is then mapped onto an equivalent one governed by a tight-binding Hamiltonian with m sites. The subspace obtained by means of the dimensionality reduction method provides a subspace which is relevant for the chiral quantum routing.

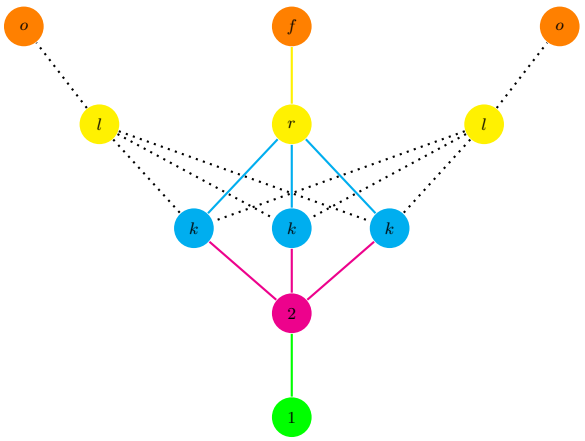

Figure 1. *Lily Graph* topology – The *input nodes* ($|1\rangle$ and $|2\rangle$) are green and magenta labeled, the *chiral layer* ($|k\rangle$), composed of d nodes, is blue labeled, the *routing layer* ($|l\rangle$ and $|r\rangle$) composed of n vertices (yellow labeled) and accordingly the n outputs ($|f\rangle$ and $|o\rangle$) are orange labeled.

The Lily graph – By engineering the topology and chirality of the graph it is possible to achieve ideal quantum rouring. To this aim we put forward the structure, termed the *Lily graph*, depicted in Fig.1. The network is defined by an input layer $\mathcal{I}$ of two nodes $|1\rangle$ and $|2\rangle$ (labeled in green and magenta, respectively), a chiral layer $\mathcal{C}$ of d vertices $|k\rangle$ (blue labeled), a routing layer $\mathcal{R}$, composed of n vertices $|l\rangle$ and $|r\rangle$ (yellow labeled) and, finally, and output layer $\mathcal{O}$ of n outputs $|o\rangle$ and $|f\rangle$ (orange labeled). The two integers d and n denote independent degrees of freedom of the topology, and may assume any value [21]. The associated Hamiltonian depends on both d and n and also on the vector of the different phases $\vec{\phi} = \{\phi_1,\phi_2,\ldots\}$, i.e. $H\left(n,d,\vec{\phi}\right)$, and is the sum of the adjacency matrices of the different layers and nodes of the discrete structure, i.e.,

$$H\left(n,d,\vec{\phi}\right) = A_{\mathcal{I}} + C_{\mathcal{C}}\left(d,\vec{\phi}\right) + C_{\mathcal{R}}\left(d,\vec{\phi},n\right) + A_{\mathcal{O}}(n), \tag{7}$$

where $A_{\mathcal{I}}$ refers to the input adjacency matrix, i.e.

$$A_{\mathcal{I}} = |1\rangle\langle 2| + |2\rangle\langle 1|, \tag{8}$$

and is associated to the *input* state $|\psi_0\rangle$. The chiral adjacency reads

$$C_{\mathcal{C}}\left(d,\vec{\phi}\right) = \sum_{k\in\mathcal{C}} e^{-i\phi_k}\,|2\rangle\langle k| + e^{i\phi_k}\,|k\rangle\langle 2|, \tag{9}$$

where the phases ϕ_k are the d roots of the unity $\sqrt[d]{1}$, i.e. $\phi_k = 2k\pi/d$. The routing adjacency $C_{\mathcal{R}}(n,d,\vec{\phi})$ is defined as

$$\begin{aligned}C_{\mathcal{R}}\left(n,d,\vec{\phi}\right) =& \sum_{k\in\mathcal{C}}\sum_{\substack{l\in\mathcal{R}\\ l\neq r}} |k\rangle\langle l| + |l\rangle\langle k| \\ &+ \sum_{k\in\mathcal{C}} e^{-i\phi_k}\,|r\rangle\langle k| + e^{i\phi_k}\,|k\rangle\langle r|.\end{aligned} \tag{10}$$

$$\tag{11}$$

Finally, the output adjacency $A_{out}(n)$ is given by

$$A_{\mathcal{I}}(n) = \sum_{l\in\mathcal{R}}\sum_{o\in\mathcal{O}} |o\rangle\langle l| + |l\rangle\langle o|, \tag{12}$$

Nearly perfect routing using only phases – The routing phenomena we want to implement are those involving an *input* state (sites $|1\rangle$, $|2\rangle$, or one of their superpositions) driven to separated spatial regions (sites $|r\rangle$, $|f\rangle$ or their superpositions, respectively), where $|r\rangle$ can be any site of the routing layer $\mathcal{R}$ and $|f\rangle$ is its associated output node. Applying the Krylov reduction method to the Hamiltonian $H\left(n,d,\vec{\phi}\right)$, starting from the vertex $|f\rangle$, we obtain the following orthonormal basis $\{|e_k\rangle\}$

$$\begin{aligned}|e_1\rangle &= |f\rangle\,, \quad |e_2\rangle = |r\rangle \\ |e_3\rangle &= \frac{1}{\sqrt{d}}\sum_{k\in\mathcal{C}} e^{i\phi_k}\,|k\rangle \\ |e_4\rangle &= |2\rangle\,, \quad |e_5\rangle = |1\rangle\end{aligned} \tag{13}$$

which is analogous to a basis that can be obtained grouping together identically evolving vertices [22], and thus providing a valid basis for the dynamics of the system. Moreover, thanks to the design of the chiral and routing layers, the effective topology, and the dimension of its Krylov representation, is independent of the number of outputs n.

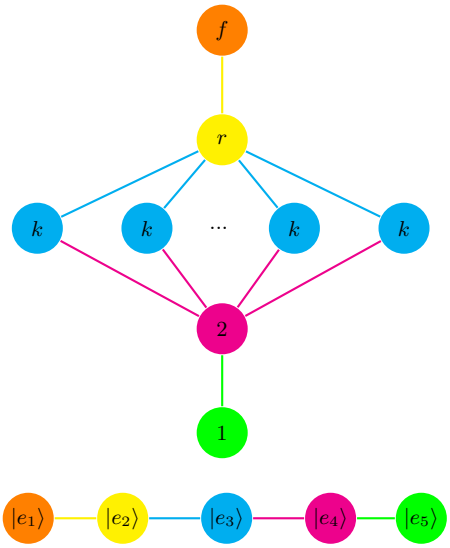

Figure 2. (Upper panel): Effective topology for the dynamics of an *input* state. The *input nodes* ($|1\rangle$ and $|2\rangle$) are green and magenta labeled, the *chiral layer* ($|k\rangle$), composed of d nodes, is blue labeled, the *routing vertex* ($|r\rangle$) is yellow labeled and the output $|f\rangle$ is orange labeled. (Lower panel): Krylov representation of the effective topology. Following the same color palette the Krylov *input vectors* $|e_5\rangle$ and $|e_4\rangle$ are green and magenta labeled, the Krylov *chiral vector* $|e_3\rangle$ is blue labeled, the Krylov *routing vector* $|e_2\rangle$ is yellow labeled and the Krylov *output vector* $|e_1\rangle$ is orange labeled

The reduced Hamiltonian in the Krylov basis is always five-dimensional, and depends on the chiral layer only through the dimension d, see Fig.2. Upon evaluating the elements $\langle e_j|\,\widetilde{H}\,|e_k\rangle$ we have the matrix representation

$$\widetilde{H} = \begin{pmatrix} 0 & 1 & 0 & 0 & 0 \\ 1 & 0 & \sqrt{d} & 0 & 0 \\ 0 & \sqrt{d} & 0 & \sqrt{d} & 0 \\ 0 & 0 & \sqrt{d} & 0 & 1 \\ 0 & 0 & 0 & 1 & 0 \end{pmatrix}. \tag{14}$$

This means that the time evolution does not depend on the overall dimensionality of the graph, and thus the routing procedure is associated to a universal time t^* valid for every number of output spatial regions n and then, for every $|\psi_f\rangle$. This is obtained because we choose the phases of the chiral layer as the roots of the unity $\sqrt[d]{1}$, such that the property

$$\sum_{k=1}^{d} e^{i\phi_k} = \sum_{k=1}^{d} e^{\frac{i2\pi k}{d}} = 0 \;\; \forall d > 1 \tag{15}$$

leads by its own to destructive interference in all the vertices $|l\rangle$ of the routing layer. We can then decide where to send the signal, e.g. to the vertex $|r\rangle$, by removing the phases through its links to the chiral layer. Looking at Fig. 1, this means that the $2 \mapsto k$ links have opposite phases compared to the $k \mapsto r$ ones, whereas all the other links $k \mapsto l$ are not chiral, mantaining the destructive effect of the chiral layer. The reduced Krylov basis guarantees that the time evolution of the system involves only the desired output state(s), since it depends only on a single site of the output (chiral) layer, and not on the others[23]. This means that for every time t the dynamics of the system does not involve the unwanted spatial regions, preventing the system from an undesired routing (see the effective graph in the upper panel of Fig. 2). Notice that in order to route the state to a different output $|r'\rangle$, it is sufficient to change the d phases of the $k \mapsto r'$ links.

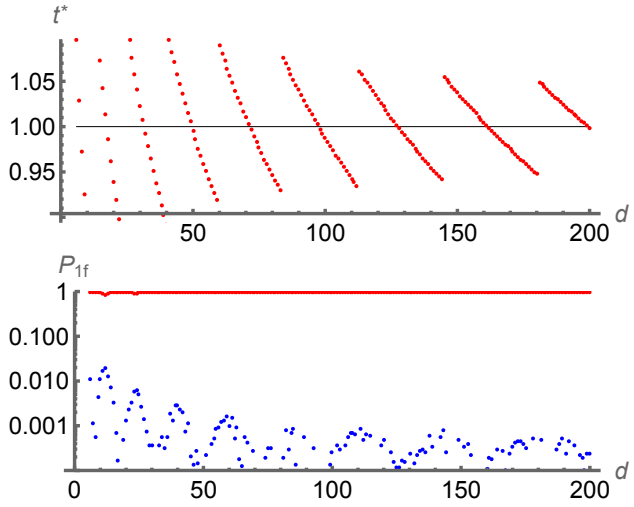

Figure 3. (Upper panel): optimal time t^* (in unit of π) maximizing the routing probability $P_{1f}(t)$ as a function of the chiral layer dimension d. (Lower panel): logplot of the maximized routing probability $P_{1f}(t^*)$ as a function of the chiral layer dimension d. We also show the difference $|P_{1f}(t^*) - P_{2r}(t^*)|$ (the curve is below 10^{-2} as far as d is larger than 15).

The two probabilities $P_{1f}(t) = \left|\langle e_1|e^{-it\widetilde{H}}|e_5\rangle\right|^2$ and $P_{2r}(t) = \left|\langle e_2|e^{-it\widetilde{H}}|e_4\rangle\right|^2$ govern the routing perfomance for localized states. Nonetheless, the condition $P_{1f}(t^*) = P_{2r}(t^*) = 1$ is a sufficient condition to obtain perfect routing also of any superposition of the states $|e_5\rangle$ and $|e_4\rangle$. Using Eq. (14), we have

$$\begin{aligned} P_{1f}(t) &= \frac{1}{4}\frac{\left[2d - (2d+1)\cos t + \cos\left(t\sqrt{1+2d}\right)\right]^2}{(1+2d)^2} \\ P_{2r}(t) &= \frac{1}{4}\left[\cos t - \cos\left(t\sqrt{1+2d}\right)\right]^2. \end{aligned} \tag{16}$$

Upon setting $t^* \simeq \pi$, we have $P_{1f}(t^*) \simeq P_{2r}(t^*)$, with

$$P_{1f}(t^*) = 1 - \frac{1-\cos\left(\pi\sqrt{2d+1}\right)}{2d} + O\left(\frac{1}{d^2}\right),$$

which is approaching 1 for increasing d (see Fig. 3). We conclude that the chiral Lily graph provides nearly perfect routing, especially for large d, in a time independent of the number of outputs and only slightly dependent on the dimension of the routing layer.

Perfect routing using chirality and edge weighting – Perfect quantum routing may be obtained by slightly modifying the Hamiltonian in Eq.(7), tuning the weights of the edges in the chiral and routing layers of the Lily graph as follows

$$H\left(n,d,\vec{\phi}\right) = A_{\mathcal{I}} + \beta\, C_{\mathcal{C}}\left(d,\vec{\phi}\right) + \beta\, C_{\mathcal{R}}\left(d,\vec{\phi},n\right) + A_{\mathcal{O}}(n)\,, \tag{17}$$

The Krylov basis is the same of Eq.(13), and the reduced Hamiltonian reads

$$\widetilde{H}(\beta) = \begin{pmatrix} 0 & 1 & 0 & 0 & 0 \\ 1 & 0 & \beta\sqrt{d} & 0 & 0 \\ 0 & \beta\sqrt{d} & 0 & \beta\sqrt{d} & 0 \\ 0 & 0 & \beta\sqrt{d} & 0 & 1 \\ 0 & 0 & 0 & 1 & 0 \end{pmatrix}, \tag{18}$$

The routing probabilities become

$$\begin{aligned} P_{1f}(\beta,t) &= \frac{1}{4}\frac{\left[2d\beta^2 - (2d+\beta^2)\cos t + \cos\left(t\sqrt{\beta^2+2d}\right)\right]^2}{(\beta^2+2d)^2} \\ P_{2r}(\beta,t) &= \frac{1}{4}\left[\cos t - \cos\left(t\sqrt{\beta^2+2d}\right)\right]^2 . \end{aligned} \tag{19}$$

By choosing $\beta\sqrt{d} = \sqrt{3/2}$ [24], we achieve perfect routing for any quantum state, i.e. $P(t^*)_{1f} = P(t^*)_{2r} = 1$, for $t^*_\beta = \pi$. The simplest realization of the Lily graph is obtained by setting $d = 2$, which requires only two phases $\phi = 0, \pi$ and setting $\beta = \sqrt{3}/2$. However, the routing time is universal, i.e. independent on n and d. Upon expanding the probabilities for times around t^*, we have

$$\begin{aligned} P_{1f}(t) &= 1 - (t-t^*_\beta)^2 + O(t-t^*_\beta)^3 \\ P_{2r}(t) &= 1 - \frac{5}{2}(t-t^*_\beta)^2 + O(t-t^*_\beta)^3\,, \end{aligned}$$

$\forall n, d$, i.e., the routing is robust against fluctuations, and the robustness is universal too.

Associated to perfect routing, the system also shows a temporal periodicity of 2π, assuring that for every time $t^*_\beta = (2q+1)\pi$ the projector condition is fulfilled, i.e.,

$$e^{-i\widetilde{H}(2q+1)\pi} = \sum_{s=0}^{4} |e_{1+s}\rangle\langle e_{5-s}|\,, \quad q \in \mathbb{N}\,.$$

Notice that the coherence (in the site basis) of the evolving states $e^{-it\widetilde{H}}|e_4\rangle$ and $e^{-it\widetilde{H}}|e_5\rangle$ is instead charaterized by a period of π. If $\beta\sqrt{d} \neq \sqrt{3/2}$ this periodicity is lost.

Conclusions – In this work, we have focused on designing a device capable of routing quantum information, initially encoded on two input nodes of a network, to n possible pairs of output nodes, which are orthogonal and mutually exclusive. Upon exploiting the formalism of continuous-time quantum walks, we have designed an optimal five-layer structure, named the Lily graph, comprising two input nodes, a chiral layer, a routing layer, and an output layer. The system's Hamiltonian has been engineered by leveraging both the chiral properties available for a quantum walker and the modulation of the graph's edge weights. The overall evolution ensures a perfect routing protocol, achieving unit fidelity, for both classical information (initially localized at a graph site) and quantum information (initially encoded in a superposition of sites). The selection of output nodes is achieved by modifying the phases of certain links in the routing layer. The time required for information transfer is universal, i.e., it does not depend on the number of outputs or the size of the chiral layer, and the overall protocol is robust, with the output fidelity being relatively unaffected by fluctuations in the interaction time.

Our results demonstrate that it is possible to achieve perfect routing of quantum information on a network characterized by a relative simplicity, and pave the way for future developments, including the routing of entanglement. The Lily graph structure provides a robust and scalable method for quantum information routing, possibly enhancing the prospects for integrating quantum technologies into existing communication and computation infrastructures.

This work has been done under the auspices of GNFM-INdAM and has been partially supported by MUR through the project PRIN22-2022T25TR3-RISQUE and by MUR and EU through the project PRIN22-PNRR-P202222WBL-QWEST.

* simone.cavazzoni@unimore.it
† giovanni.ragazzi@unimore.it
‡ paolo.bordone@unimore.it
§ matteo.paris@fisica.unimi.it

[1] M.-H. Yung and S. Bose, Physical Review A **71**, 032310 (2005).
[2] A. Zwick, G. A. Alvarez, J. Stolze, and O. Osenda, Physical Review A **84**, 022311 (2011).
[3] V. M. Kendon and C. Tamon, Journal of Computational and Theoretical Nanoscience **8**, 422 (2011).
[4] I. Shomroni, S. Rosenblum, Y. Lovsky, O. Bechler, G. Guendelman, and B. Dayan, Science **345**, 903 – 906 (2014).
[5] J. Lu, L. Zhou, L.-M. Kuang, and F. Nori, Physical Review A - Atomic, Molecular, and Optical Physics **89**,

013805 (2014).
[6] G. M. Nikolopoulos, I. Jex, *et al.*, *Quantum state transfer and network engineering* (Springer, 2014).
[7] M. Caleffi, IEEE Access **5**, 22299 – 22312 (2017).
[8] F. Petiziol, E. Arimondo, L. Giannelli, F. Mintert, and S. Wimberger, Scientific reports **10**, 2185 (2020).
[9] S. Paganelli, S. Lorenzo, T. J. G. Apollaro, F. Plastina, and G. L. Giorgi, Physical Review A **87**, 062309 (2013).
[10] S. Sazim, V. Chiranjeevi, I. Chakrabarty, and K. Srinathan, Quantum Information Processing **14**, 4651 (2015).
[11] M. Pant, H. Krovi, D. Towsley, L. Tassiulas, L. Jiang, P. Basu, D. Englund, and S. Guha, npj Quantum Information **5**, 25 (2019).
[12] B. Chen, Y.-Z. He, T.-T. Chu, Q.-H. Shen, J.-M. Zhang, and Y.-D. Peng, Progress of Theoretical and Experimental Physics **2020**, 053A01 (2020).
[13] A. Bottarelli, M. Frigerio, and M. G. Paris, AVS Quantum Science **5** (2023).
[14] M. S. Underwood and D. L. Feder, Physical Review A **85**, 052314 (2012).
[15] S. Apers, S. Chakraborty, L. Novo, and J. Roland, Phys. Rev. Lett. **129**, 160502 (2022).
[16] D. Lu, J. D. Biamonte, J. Li, H. Li, T. H. Johnson, V. Bergholm, M. Faccin, Z. Zimboràs, R. Laflamme, J. Baugh, and S. Lloyd, Physical Review A **93**, 042302 (2016).
[17] M. Frigerio, C. Benedetti, S. Olivares, and M. G. A. Paris, Physical Review A **104**, L030201 (2021).
[18] A. Khalique, A. Sett, J. Wang, and J. Twamley, New Journal of Physics **23** (2021).
[19] F. Caruso, A. W. Chin, A. Datta, S. F. Huelga, and M. B. Plenio, The Journal of Chemical Physics **131**, 09B612 (2009).
[20] L. Novo, S. Chakraborty, M. Mohseni, H. Neven, and Y. Omar, Scientific reports **5**, 1 (2015).
[21] Strictly speaking the chiral parameter must be greater than one ($d > 1$) since to create interference the input wave-function must be split in at least 2 separated spatial regions.
[22] D. A. Meyer and T. G. Wong, Physical review letters **114**, 110503 (2015).
[23] F. Thiel, I. Mualem, D. Meidan, E. Barkai, and D. A. Kessler, Phys. Rev. Res. **2**, 043107 (2020).
[24] Or any β solution of the equation $\sqrt{2\beta^2+1} = 2q$, with $q \in \mathbb{N}$.